Accuracy of Integration of Dental Cast and Cephalograms Compared with Cone-Beam Computed Tomography: A Comparative Study

Fanfan Dai
Peking University School and Hospital of Stomatology
Si Chen
Peking University School and Hospital of Stomatology
Tingting Feng
The Affiliated Stomatology Hospital of Tongji University
Gui Chen
Peking University School and Hospital of Stomatology
Jiuhui Jiang
Peking University School and Hospital of Stomatology
Ruoping Jiang
Peking University School and Hospital of Stomatology
Jiuxiang Lin
Peking University School and Hospital of Stomatology
Bing Han (kqbinghan@bjmu.edu.cn)
Peking University School and Hospital of Stomatology
Tianmin Xu
Peking University School and Hospital of Stomatology

Research Article

Keywords: Orthodontic, Dental cast, Cephalograms, Cone-beam computed tomography, Registration

Posted Date: June 22nd, 2021

DOI: https://doi.org/10.21203/rs.3.rs-586322/v1

Abstract

Background: This study proposes a method that integrates maxillary dental cast and cephalograms and evaluates its accuracy compared with cone-beam computed tomography (CBCT) scans.

Methods: The study sample comprised 20 adult patients with records of dental casts, cephalograms, and craniofacial CBCT scans. The maxillary dental cast was integrated with lateral and frontal cephalograms based on best-fit registration of palatal and dental outline curves from dental cast with cephalogram tracings. Linear measurement was conducted to assess the intra- and inter-examiner reproducibility of the proposed intergration method using intraclass correlation coefficients; linear and angular measurements were conducted to assess its accuracy with CBCT scans as a standard reference. Paired t test, one sample t test, and mean ± standard deviation of the absolute value of difference were used to compare the integrated images and CBCT.

Results: The integration method showed good intra- and inter-examiner reproducibility (intraclass correlation coefficients >0.98). The differences in linear and angular measurements between the integrated images and CBCT were not statistically significant but with a large deviation. When absolute value of difference was computed, the linear distance error was 0.51 ± 0.34 mm, the tooth point coordinate errors in *X*, *Y* and *Z* axis were 0.22 ± 0.22, 0.38 ± 0.32 and 0.21 ± 0.21mm respectively; the angular error in pitch, roll and yaw of the dental cast was 0.82 ± 0.51, 0.92 ± 0.59 and 0.80 ± 0.41 degree respectively.

Conclusions: The proposed method for integration of dental cast and cephalograms showed good reproducibility and acceptable accuracy compared with CBCT. It could be helpful for researchers to study three-dimensional tooth growth changes using the existing craniofacial growth data especially cephalograms.

Background

Orthodontists are concerned about tooth movement during growth, which is crucial in orthodontic treatment planning and therapeutic effect evaluation. Our knowledge about tooth growth changes attributes to the precious growth samples in several Growth Study Centers. Sagittal growth changes in maxillary first molars and incisors have been widely studied using lateral cephalograms with the Bjork implant sample [1–3], the Matthews implant sample [4, 5], a sample from the Bolton-Brush Growth Study Center [6], and one from the Burlington Growth Center [7]. Moreover, transverse growth changes in molars have been studied using dental casts with the sample from the Iowa Facial Growth Study [8, 9], and inclination of canines and premolars has been studied using panoramic radiographs with a cross-sectional growth sample [10].

Entering the three-dimensional (3D) digital era, orthodontists are focusing on 3D evaluation of tooth movement. 3D tooth treatment changes can be measured through superimposition of pre- and post-treatment CBCT scans [11] or digital dental casts [12–14]. However, knowledge regarding 3D tooth

growth changes is difficult to study. Firstly, the collection of longitudinal craniofacial growth data in terms of annual CBCT scans would be challenging considering ethical issues regarding radiation exposure; secondly, digital dental cast superimposition based on palatal vault region does not apply to growing individuals as the palatal vault region is not stable for registration [15].

The existing longitudinal craniofacial growth data from most Growth Study Centers include only plaster dental casts and two-dimensional (2D) cephalograms. Although results from previous 2D studies on sagittal and transverse growth changes in teeth could be integrated together, inconsistency of study methods, i.e., use of lateral cephalograms for sagittal evaluation, panoramic radiographs for tooth inclination, and dental casts for transverse evaluation, could not give an intuitive perception of 3D tooth movement. So integration of cephalograms and dental casts into a new 3D dentoskeletal model may give solution to 3D tooth growth study.

In order to assess the 3D position of teeth relative to craniofacial structures, certain studies have proposed the integration of digital dental casts and cephalograms through tie points or the projected occlusal line of dentition [16–18]. Baumrind et al suggested that by using a combination of this integration method with the classical superimposition of lateral cephalograms, 3D dental casts from more than one time point can be expressed as a common frame of reference for longitudinal studies of treatment outcomes or growth through time [17]. However, the accuracy of integration of digital dental casts and cephalograms has not yet been verified.

Therefore, the present study aimed to evaluate the accuracy of integration of digital dental casts and cephalograms with CBCT data as a standard reference. If the error of the integration method is acceptable, the existing longitudinal craniofacial growth sample could then be used to explore 3D tooth growth changes with indirect digital dental cast superimposition— a combination of the integration method and superimposition of lateral cephalograms.

Methods

Twenty adult patients (10 male, 10 female),aged 18 to 30 years, were searched and selected from the patient database in the Department of Orthodontics at our hospital and enrolled in this study. Patients had common pretreatment orthodontic records of plaster dental casts, panoramic radiograph and lateral and frontal cephalograms, and took additional craniofacial CBCT examinations within one month because of the need of orthognathic surgery. The study procedure was shown in Fig. 1.

Plaster dental casts were scanned by a laser scanner (3Shape R700, 3Shape A/S, Copenhagen, Denmark), the scanned images were reconstructed into 3D digital dental casts. Lateral and frontal cephalograms were obtained from the same Cephalostat (OC-100, Instrumentarium Imaging Co., Finland); the patient turned 90° while the Cephalostat was fixed between two scans. Craniofacial CBCT images were acquired using a CBCT unit (NewTom VG, Quantitative Radiology, Verona, Italy) with the following parameters: 15×15 cm FOV, 110 kVp, 10.8 mA, 3.6 s, and 0.3-mm slice thickness.

The cephalograms were digitally traced using Adobe Photoshop CS 5.0 (Adobe Systems Corporation, San Jose, CA, USA) on a hand-writable liquid crystal display (Cintiq DTK-1300, Wacom, Saitama, Japan) (Fig. 2a). The tracings were saved in BMP format. By using the Matlab 10.0 (Math Works Inc., Mass., USA) with a self-edited code (see Additional file 1), the tracings were adjusted by magnification, extracted as 2D points, and then transformed into 3D points by adding an additional *Z* value of zero to the lateral cephalogram tracing and an additional *X* value of zero to the frontal cephalogram tracing. The final 3D tracings were saved in TXT format and imported into the Rapidform 2006 software (Inus Techonology, Seoul, Korea), where the lateral and frontal cephalogram tracings were presented in the *XY* and *YZ* planes respectively, and intersected with each other at the facial midline of the frontal tracing.

Then, the maxillary digital dental cast was imported into the Rapidform software to integrate with the cephalogram tracings. First, the midsagittal plane of the maxillary digital dental cast, generated as the mirror symmetry plane of the palatal vault region, was coincided with the *XY* plane; subsequently, the inferior outline of the palate (Outline_P) was generated by slicing the digital cast with the *XY* plane. The labial outline of the anterior incisor (Outline_I) and the occlusal outline of the dentition (Outline_O1) were generated by projecting the cast onto the *XY* plane, while the buccal outline of the second molar (Outline_M) and the occlusal outline of the dentition (Outline_O2) were generated by projecting the cast onto the *YZ* plane (Fig. 2b). Thereafter, the maxillary dental cast was registered with lateral and frontal cephalogram tracings through 3D translation and rotation, where the digital dental cast was first aligned laterally, then frontally, going back and forth between two cephalograms until radiographic tracings and dental cast outlines of teeth and palate were best-fit registered [18]. The best-fit registration was defined as follows: (i) on the *XY* plane, Outline_I and Outline_O1 coincided with corresponding lateral cephalogram tracings, Outline_P was just below the corresponding palatal tracing; (ii) on the *YZ* plane, Outline_M and Outline_O2 coincided with corresponding frontal cephalogram tracings (Fig. 2c).

Figure 2d shows the final integration of the maxillary dental cast and the cephalograms. The mandibular dental cast could be integrated through its occlusion with maxillary dental cast. Subsequently, measurements were recorded to evaluate the accuracy and reproducibility of this method. Nasion (N), ANS, and PNS points were selected on the lateral cephalogram, and PP line was constructed by connecting ANS and PNS. The mesiobuccal cusps of bilateral second molars (UM_R and UM_L) and midpoint of the incisal edge of the right central incisor (UI_R) were selected on the dental cast (Fig. 3a). The N point was set as the origin of coordinates and the PP line as the direction of the *X*-axis, the 3D coordinate values (*X*, anteroposterior; *Y*, vertical; *Z*, mediolateral) of UM_R, UM_L, and UI_R points were recorded, and their distance from N point and PP line were measured as UM_R-N, UM_L-N, and UI_R-N and UM_R-PP, UM_L-PP, and UI_R-PP, respectively. The integration process and measurements were repeated two times at a 2-week interval by two examiners.

As the standard reference, CBCT images were processed using the Dolphin imaging software (Version 11.7, Dolphin Imaging & Management Systems, CA, USA). First, the skull was oriented with the Frankfort horizontal plane parallel to the ground and the midsagittal plane passing through the N, sella, and basion

points [19]. Subsequently, the landmarks of N, ANS, and PNS were located on the midsagittal plane (Fig. 3b), whereas those of UM_R, UM_L, and UI_R were identified on the three orthogonal planes (Fig. 3c); the original coordinates of the six points were exported and this was followed by the same measurements of distances and point coordinates as recorded in the integrated images. The distance measurement and point coordinate transformation were completed using the Matlab with a self-edited code (see Additional file 2).

To evaluate the angular error of the integration method, the pitch, roll and yaw [20] of the dental cast in the integrated images compared with the CBCT were measured. First, 3D surface skeletal model was generated from CBCT scans using Dolphin software. Second, the skeletal model was imported into the Rapidform software and registered with the integrated images, where the midsagittal plane (mirror symmetry plane) of the skeletal model coincided with the *XY* plane initially (Fig. 4a) and then the sliced and projected outline curves conincided with the lateral and frontal cephalogram tracings through 3D translation and rotation (Fig. 4b-c). Subsequently, a copied dental cast was superimposed with the skeletal model through registration of crown surfaces of all teeth (Fig. 4d-e). Thereafter, the deviation of the cephalogram-integrated dental cast from the CBCT-superimposed dental cast in terms of pitch, roll and yaw was measured as rotation angle around *Z*, *X* and *Y* axes respectively (Fig. 4f).

Statistical analysis

We performed the statistical analysis using SPSS software (version 26.0; IBM, Armonk, NY). Intra- and inter-examiner reproducibility of the method for integration of the digital dental cast and cephalograms were tested using intraclass correlation coefficients (ICCs) with a 95% confidence interval. All data were determined to have normal distributions as assessed with the Kolmogorov-Smirnov test. Comparsions of linear distance and coordinate values (*X, Y* and *Z*) between the integrated and the CBCT images were conducted with paired t test; comparsions of angular measurements (pitch, roll and yaw) were conducted with one sample t test. The difference and the absolute value of the difference were both described as mean ± standard devitation.

Results

The ICCs of intra- and inter-examiner measurements were > 0.98 for all linear distance measurements (Table 1), which indicated good reproducibility of the integration method. Tables 2 to 4 summarizes data regarding accuracy of the integration method. Differences in distance measurements between the integrated and the CBCT images were not statistically significant, with the average difference of − 0.08 ± 0.61 mm. When the absolute value of the difference was considered, the average difference was 0.51 ± 0.34 mm. Differences in tooth point coordinate values were not statistically significant for all *X*, *Y* and *Z* axes, with the average difference of − 0.02 ± 0.31 mm, 0.08 ± 0.49 mm and − 0.08 ± 0.29 respectively. The average differences were 0.22 ± 0.22 mm, 0.38 ± 0.32 mm and 0.21 ± 0.21mm, respectively, when absolute value of the difference was calculated. Pitch, roll and yaw of the dental cast in the integrated images compared with CBCT were − 0.41 ± 0.89, − 0.15 ± 1.10 and 0.04 ± 0.91 degree, respectively, which

showed no statistically significant. Pitch, roll and yaw were 0.82 ± 0.51, 0.92 ± 0.59 and 0.80 ± 0.41 degree, respectively, when the absolute value was computed.

Table 1
The intraclass correlation coefficients of distance measurements in the integrated images

Measurements	Examiner 1		Examiner 2		Between examiners	
	ICC	95%CI	ICC	95%CI	ICC	95%CI
UM_R-N	0.998	0.995,0.999	0.997	0.993,0.999	0.996	0.954,0.999
UM_L-N	0.996	0.991,0.999	0.997	0.993,0.999	0.997	0.993,0.999
UI_R-N	0.997	0.993,0.999	0.997	0.992,0.999	0.997	0.993,0.999
UM_R-PP	0.999	0.997,0.999	0.993	0.982,0.997	0.988	0.958,0.996
UM_L-PP	0.997	0.993,0.999	0.989	0.973,0.996	0.988	0.969,0.995
UI_R-PP	0.998	0.994,0.999	0.990	0.974,0.996	0.995	0.988,0.998

Table 2
Measurement differences in 3D linear distance between integrated images and CBCT images (mm)

Distances	CBCT	Integrated images	Difference 1*	P value[&]	Difference 2[#]
UM_R-N	87.18 ± 6.11	86.83 ± 6.03	-0.34 ± 0.34		0.38 ± 0.30
UM_L-N	87.00 ± 5.33	86.89 ± 5.26	-0.11 ± 0.65		0.56 ± 0.32
UI_R-N	84.33 ± 4.54	84.60 ± 4.67	0.27 ± 0.56		0.54 ± 0.29
UM_R-PP	38.30 ± 3.03	37.83 ± 3.07	-0.47 ± 0.56		0.62 ± 0.38
UM_L-PP	38.11 ± 2.80	38.13 ± 2.86	0.02 ± 0.66		0.53 ± 0.38
UI_R-PP	29.43 ± 2.53	29.62 ± 2.64	0.19 ± 0.53		0.44 ± 0.33
Average			-0.08 ± 0.61	0.171	0.51 ± 0.34
[&], P < 0.05 indicates statistically significant.					
*, Difference 1 indicates difference considering positive and negative value.					
[#], Difference 2 indicates absolute value of difference.					

Table 3
Measurement differences in 3D coordinate values of UM_R, UM_L, and UI_R between integrated images and CBCT images (mm)

Points	CBCT	Integrated images	Difference 1*	P value[&]	Difference 2[#]
UM_R-*X*	-26.66 ± 7.52	-26.65 ± 7.54	0.01 ± 0.28		0.19 ± 0.20
UM_L-*X*	−27.20 ± 6.34	−27.22 ± 6.30	−0.02 ± 0.39		0.29 ± 0.25
UI_R-*X*	10.75 ± 5.30	10.69 ± 5.33	−0.06 ± 0.26		0.17 ± 0.20
Average-*X*			-0.02 ± 0.31	0.534	0.22 ± 0.22
UM_R-*Y*	-76.68 ± 5.92	-76.31 ± 5.86	0.36 ± 0.35		0.41 ± 0.29
UM_L-*Y*	-76.35 ± 5.12	-76.28 ± 5.15	0.07 ± 0.55		0.44 ± 0.33
UI_R-*Y*	−83.35 ± 4.61	−83.54 ± 4.72	−0.19 ± 0.41		0.30 ± 0.33
Average-*Y*			0.08 ± 0.49	0.211	0.38 ± 0.32
UM_R-*Z*	30.83 ± 2.94	30.73 ± 2.96	−0.10 ± 0.35		0.25 ± 0.25
UM_L-*Z*	−30.95 ± 2.18	−31.01 ± 2.16	−0.06 ± 0.34		0.24 ± 0.25
UI_R-*Z*	4.54 ± 1.11	4.46 ± 1.19	−0.09 ± 0.16		0.15 ± 0.10
Average-*Z*			-0.08 ± 0.29	0.039	0.21 ± 0.21
[&], P < 0.05/3 indicates statistically significant (Bonferroni adjustment).					
*, Difference 1 indicates difference considering positive and negative value.					
[#], Difference 2 indicates absolute value of difference.					

X, anteroposterior; *Y*, vertical; *Z*, mediolateral.

Table 4
Angular errors in terms of pitch, roll and yaw of the maxillary dental cast within the integrated images compared with CBCT (degree).

Angular error	Difference 1*	P value[&]	Difference 2[#]
Pitch	-0.41 ± 0.89	0.053	0.82 ± 0.51
Roll	-0.15 ± 1.10	0.554	0.92 ± 0.59
Yaw	0.04 ± 0.91	0.841	0.80 ± 0.41
[&], P < 0.05/3 indicates statistically significant (Bonferroni adjustment).			
*, Difference 1 indicates difference considering positive and negative value.			
[#], Difference 2 indicates absolute value of difference.			

Discussion

3D growth changes in teeth can be explored by superimposing dental casts. The medial palatal rugae points were demonstrated relatively stable and suggested as reference points for superimposing dental cast in longitudinal dental analysis [21–23]. However, these studies were based on anteroposterior and transverse linear measurements, Christou et al [15] found vertical displacement of the palatal ruage in adolescents. The problem in establishing a stable palatal region as that described by Jang et al [12] and Chen et al [13] for direct dental cast superimposition has not been clearly solved in growing subjects. Thus, the present study proposed a novel method for integration of maxillary digital dental cast and cephalograms and evaluate its accuracy with the CBCT as reference; then, combine the integration method with maxillary structural superimposition of lateral cephalograms, indirect maxillary dental cast superimposition could be achieved to study 3D tooth growth changes.

Methods for integration of digital casts and cephalograms have been studied through registration of occlusal outlines [17, 18]. Through 3D translation and rotation, digital dental casts were first aligned laterally, then frontally, going back and forth between two cephalograms until radiographic outlines of teeth and surface images of dental casts were superimposed [18]. Our study used a similar integration method with common software. Moreover, as detailed occlusal outlines may not be clearly traceable owing to image overlap of intercuspation, Outline_P, defined just below the corresponding palatal tracing of the lateral cephalogram since the dental cast had a thin layer of palatal mucosa along the midpalatal suture [24], was supplemented for best-fit registration.

The integration method proposed by Baumrind et al. and Hans et al. has not been validated yet. Hence, the accuracy of integrated images of digital dental casts and cephalograms can be evaluated with CBCT data as a standard reference. In the present study, 3D measurements of integrated and CBCT images were compared. Though CBCT itself had errors in 3D measurements, it was most commonly used 3D craniofacial data in orthodontic research [25]. Skeletal landmarks on the midsagittal plane and dental

landmarks of crown tips were used since they were readily accessible and demonstrated greater consistency [26]. Measurements of UM_R-N, UM_L-N, and UI_R-N and UM_R-PP, UM_L-PP, and UI_R-PP were used to determine spatial positions of UM_R, UM_L, and UI_R points relative to the N point and PP line, respectively (i.e., the digital dental cast relative to the lateral cephalogram). Based on our results, the average difference between integrated and CBCT images showed no statistical significance. However, the standard deviation was large. If the absolute value of the difference was computed, the average difference was 0.51 ± 0.34 mm. An error of 0.5 mm for linear measurement was considered acceptable in research.

The error in *XYZ* coordinates of tooth under the coordinate system generated from craniofacial structure was another term of linear measurement error which showed the error in tooth displacement more visually. When decomposed to *XYZ* coordinates, the differences were not statistically significant in all values. Similarly, the standard deviation was obviously larger than the mean value. If the absolute value of the difference was computed, the average differences were 0.22 ± 0.22, 0.38 ± 0.32 and 0.21 ± 0.21 mm, respectively, in *X*, *Y* and *Z* axes. A larger error in *Y* axis may result from the inaccurate occlusal outline tracing owing to image overlap of intercuspation and the inaccurate palatal outline registration due to a thin layer of palatal mucosa along the midpalatal suture [24].

In order to evaluate angular error of the integration method compared with CBCT, registration of CBCT with cephalograms and registration of dental cast with CBCT were done sequentially, this made the cephalogram-integrated dental cast and CBCT-superimposed dental cast being under the mutual coordinate system. Therefore, the angular error of the integration method was presented as pitch, roll and yaw of the cephalogram-integrated dental cast relative to the CBCT-superimposed dental cast. The results showed no statistically significant difference. When the absolute value of angle was computed, the pitch, roll and yaw were all no more than 1 degree, which was considered acceptable in research. Moreover, considering that errors also existed in registrations of CBCT with cephalograms and dental cast with CBCT [27, 28], the error in integration of dental cast with cephalograms would be even smaller.

Mandibular dental cast could be integrated with the cephalograms just through its occlusion with the maxillary dental cast. This method of integration of dental casts and cephalograms is not for replacement of taking a CBCT since the latter provides more information, but for reuse of the existing and irreproducible growth samples in the Growth Study Centers to do available 3D growth study. Combine the integration method with maxillary structural superimposition of lateral cephalograms, indirect maxillary dental cast superimposition could be achieved to study 3D maxillary tooth growth changes. Similarly, 3D growth changes in mandibular teeth can be explored using indirect mandibular dental cast superimposition—a combination of the integration method with mandibular lateral cephalogram superimposition. However, the integration method is now manipulated manually and time-consuming, it would be more practical if done by computer automatically in the future.

Reasearch Application

The existing Craniofacial Growth Centers had longitudinal records of plaster dental casts and frontal and lateral cephalograms. Combine the integration of maxillary dental cast and cephalograms with maxillary structural superimposition of lateral cephalograms, indirect maxillary dental cast superimposition could be achieved to study 3D tooth growth changes.

Figure 5 shows a subject from the growth sample who had annual records from 13 to 17 years old. For each time point of the subject, the corresponding maxillary dental cast and the cephalograms were integrated using the method described earlier. In addition, by using the maxillary structural superimposition method [2], lateral cephalogram tracings of age 14 to age 17 were superimposed with those of age 13 (Fig. 5a). Thereafter, indirect superimposition of maxillary dental casts of the five time points was achieved (Fig. 5b). Under the mutual coordinate system, 3D displacements and angular changes of every single tooth could be measured to evaluate tooth growth changes.

Conclusion

Integration of digital dental cast and cephalograms demonstrated favorable reproducibility and accuracy. By combining the integration method with structural superimposition of lateral cephalograms, indirect dental cast superimposition could be achieved, and which will be very valuable for the Craniofacial Growth Centers all over the world to explore 3D tooth growth changes using the existing sample data.

Abbreviations

CBCT, cone-beam computed tomography; 3D, three-dimensional; 2D, two-dimensional; N, nasion; ANS, anterior nasal spine; PNS, posterior nasal spine; UM_R, mesiobuccal cusp of right second molar; UM_L, mesiobuccal cusp of left second molar; UI_R, midpoint of the incisal edge of the right central incisor; ICC, intraclass correlation coefficients.

Declarations

Ethics approval and consent to participate

This study was approved by the Ethics Committee of the Peking University School and Hospital of Stomatology (PKUSSIRB-201626009). Written informed consent was obtained from all patients involved in the study.

Consent for publication

Not applicable.

Availability of data and material

The datasets used and analyzed during the current study are available from the corresponding author on reasonable request.

Competing interests

The authors declare that they have no competing interests.

Funding

This work was supported by the International Science & Technology Cooperation Program of China (grant No. 2014DFA31800), National Nature Science Foundation of China (grant No. 82071172, 51972005, 51672009), Beijing Natural Science Foundation (grant No. 7192227) and Beijing Municipal Science and Technology Commission (No. Z181100001718112) in the design of the study and collection, analysis, and interpretation of the data and in writing the manuscript.

Authors' contributions

BH and TX designed the experiments. JJ, RJ and JL provided the sample. FD and TF executed the experiments. FD analyzed the data and wrote the manuscript. SC and GC made critical revision. All authors read and approved the final manuscript.

Acknowledgments

We thank M.C. Yu (Center of Information Science, School of Electronics Engineering and Computer Science, Peking University) for MATLAB programming.

References

1. Bjork A, Skieller V. Facial development and tooth eruption. An implant study at the age of puberty. Am J Orthod. 1972;62:339–83.
2. Bjork A, Skeller V. Postnatal growth and development of the maxillary complex. In: McNamara JA Jr, editor. Factors affecting the growth of the midface, Monograph 6, Craniofacial Growth Series. Ann Arbor: Center for Human Growth and Development, University of Michigan; 1976. p. 61–9.
3. Iseri H, Solow B. Continued eruption of maxillary incisors and first molars in girls from 9 to 25 years, studied by the implant method. Eur J Orthod. 1996;18:245–56.
4. Nielsen IL. Maxillary superimposition: a comparison of three methods for cephalometric evaluation of growth and treatment change. Am J Orthod Dentofacial Orthop. 1989;95:422–31.
5. Baumrind S, Ben-Bassat Y, Bravo LA, Curry S, Korn EL. Partitioning the components of maxillary tooth displacement by the comparison of data from three cephalometric superimpositions. Angle Orthod. 1996;66:111–24.
6. Tsourakis AK, Johnston LE. Class II malocclusion: The aftermath of a "perfect storm". Semin Orthod. 2014;20:59–73.
7. Martinelli FL, de Oliveira Ruellas AC, de Lima EM, Bolognese AM. Natural changes of the maxillary first molars in adolescents with skeletal Class II malocclusion. Am J Orthod Dentofacial Orthop.

2010;137:775–81.

8. Marshall S, Dawson D, Southard KA, Lee AN, Casko JS, Southard TE. Transverse molar movements during growth. Am J Orthod Dentofacial Orthop. 2003;124:615–24.
9. Hesby RM, Marshall SD, Dawson DV, Southard KA, Casko JS, Franciscus RG, et al. Transverse skeletal and dentoalveolar changes during growth. Am J Orthod Dentofacial Orthop. 2006;130:721–31.
10. Alessandri-Bonetti G, Incerti-Parenti S, Garulli G, Gatto MR, Visconti L, Paganelli C. Maxillary first premolar inclination in 8- to 11-year-old children: an observational cross-sectional study on panoramic radiographs. Am J Orthod Dentofacial Orthop. 2016;149:657–65.
11. Yatabe M, Prieto JC, Styner M, Zhu H, Ruellas AC, Paniagua B, et al. 3D superimposition of craniofacial imaging—The utility of multicentre collaborations. Orthod Craniofac Res. 2019;22 Suppl 1:213–20.
12. Jang I, Tanaka M, Koga Y, Iijima S, Yozgatian JH, Cha BK, et al. A novel method for the assessment of three-dimensional tooth movement during orthodontic treatment. Angle Orthod. 2009;79:447–53.
13. Chen G, Chen S, Zhang XY, Jiang RP, Liu Y, Shi FH, et al. Stable region for maxillary dental cast superimposition in adults, studied with the aid of stable miniscrews. Orthod Craniofac Res. 2011;14:70–9.
14. Park TJ, Lee SH, Lee KS. A method for mandibular dental arch superimposition using 3D cone beam CT and orthodontic 3D digital model. Korean J Orthod. 2012;42:169–81.
15. Christou P, Kiliaridis S. Vertical growth-related changes in the positions of palatal rugae and maxillary incisors. Am J Orthod Dentofacial Orthop. 2008;133:81–6.
16. Curry S, Baumrind S, Carlson S, Beers A, Boyd R. Integrated three-dimensional ciraniofacial mapping at the Craniofacial Research Instrumentation Laboratory/University of the Pacific. Semin Orthod. 2001;7:258–65.
17. Baumrind S, Carlson S, Beers A, Curry S, Norris K, Boyd RL. Using three-dimensional imaging to assess treatment outcomes in orthodontics: a progress report from the University of the Pacific. Orthod Craniofac Res. 2003;6 Suppl 1:132–42.
18. Hans MG, Palomo JM, Dean D, Cakirer Banu, Min KJ, Han S, et al. Three-dimensional imaging: The Case Western Reserve University method. Semin Orthod. 2001;7:233–43.
19. Kim HJ, Kim BC, Kim JG, Zhengguo P, Kang SH, Lee SH. Construction and validation of the midsagittal reference plane based on the skull base symmetry for three-dimensional cephalometric craniofacial analysis. J Craniofac Surg. 2014;25:338–42.
20. Ackerman JL, Proffit WR, Sarver DM, Ackerman MB, Kean MR. Pitch, roll, and yaw: Describing the spatial orientation of dentofacial traits. Am J Orthod Dentofacial Orthop. 2007;131:305–10.
21. Almeida MA, Phillips C, Kula K, Tulloch C. Stability of the palatal rugae as landmarks for analysis of dental casts. Angle Orthod. 1995;65:43–8.

22. Hoggan BR, Sadowsky C. The use of palatal rugae for the assessment of anteroposterior tooth movements. Am J Orthod Dentofacial Orthop. 2001;119:482–8.
23. Kim HK, Moon SC, Lee SJ, Park YS. Three-dimensional biometric study of palatine rugae in children with a mixed-model analysis: A 9-year longitudinal study. Am J Orthod Dentofacial Orthop. 2012;141:590–7.
24. Kim HJ, Yun HS, Park HD, Kim DH, Park YC. Soft-tissue and cortical-bone thickness at orthodontic implant sites. Am J Orthod Dentofacial Orthop. 2006;130:177–82.
25. Pittayapat P, Bornstein MM, Imada TSN, Coucke W, Lambrichts I, Jacobs R. Accuracy of linear measurements using three imaging modalities: two lateral cephalograms and one 3D model from CBCT data. Europ J Orthod. 2015;37:202–8.
26. Sam A, Currie K, Oh H, Flores-Mir C, Lagravere-Vich M. Reliability of different three-dimensional cephalometric landmarks in cone-beam computed tomography: A systematic review. Angle Orthod. 2019;89:317–32.
27. Noh H, Nabha W, Cho JH, Hwang HS. Registration accuracy in the integration of laser-scanned dental images into maxillofacial cone-beam computed tomography images. Am J Orthod Dentofacial Orthop. 2011;140:585–91.
28. Sun LJ, Hwang HS, Lee KM. Registration area and accuracy when integrating laser-scanned and maxillofacial cone-beam computed tomography images. Am J Orthod Dentofacial Orthop. 2018;153:355–61.

Figures

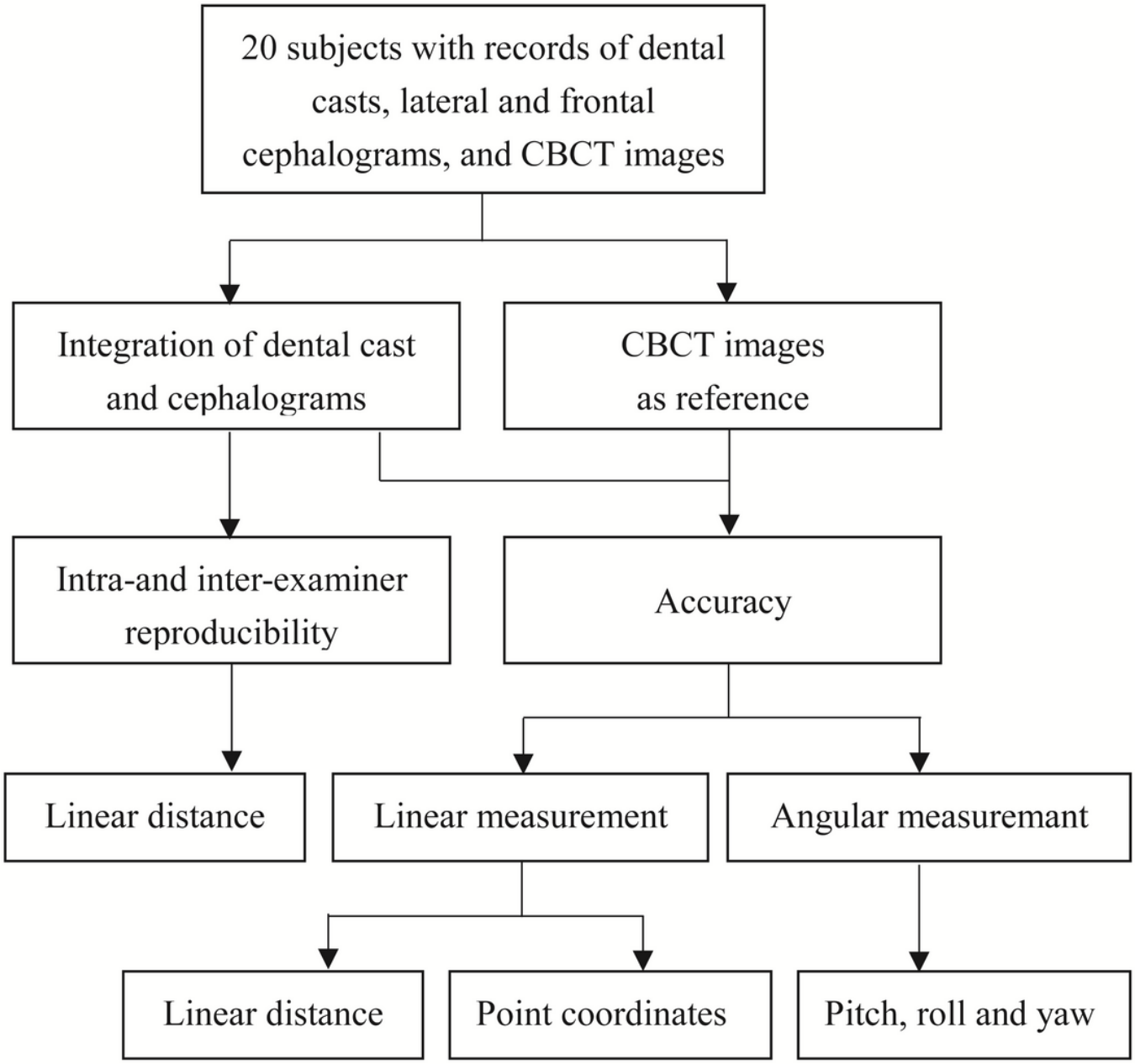

Figure 1

Study flow chart

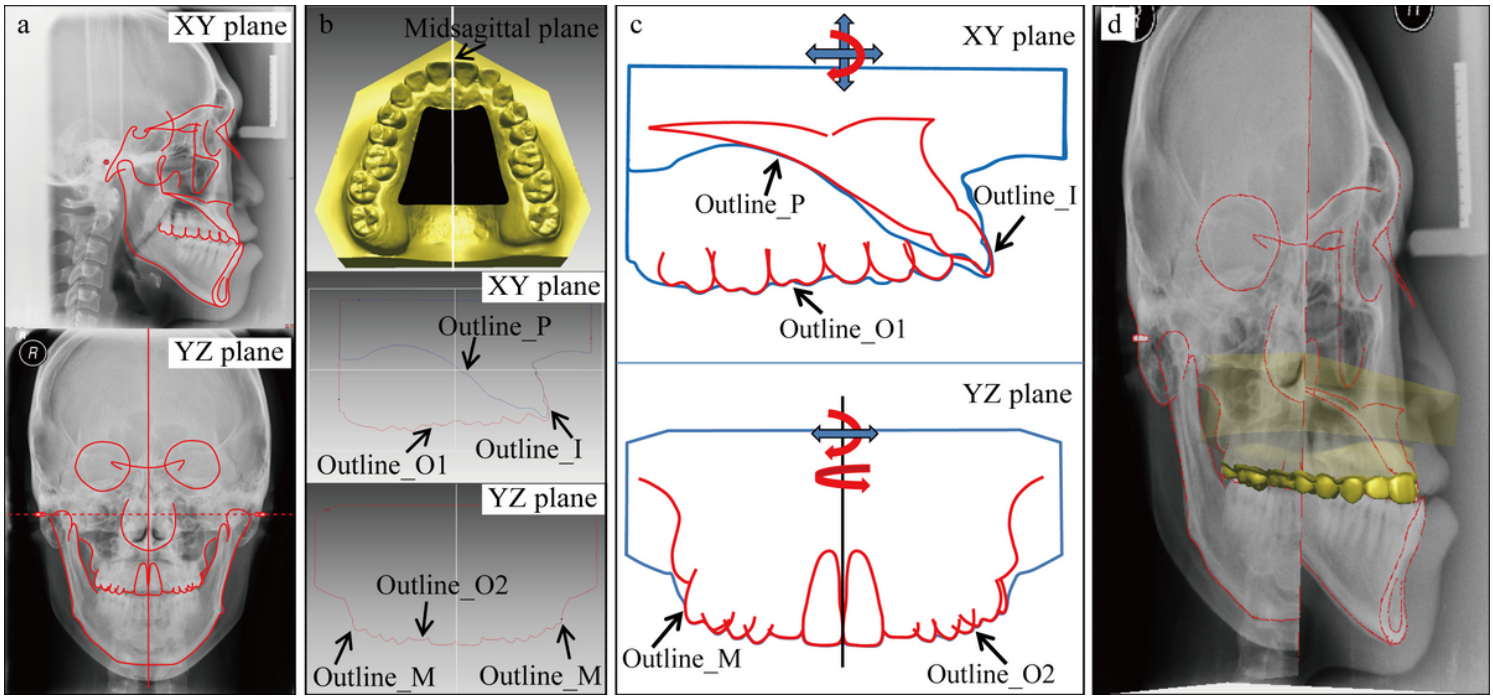

Figure 2

Integraion of dental cast and cephalograms. a Cephalometric tracings on XY and YZ planes. b Midsagittal plane of the palatal vault region (dark), and dental cast outlines on XY and YZ planes. c Best-fit registration between cephalometric tracings (red) and dental cast outlines (blue) through 3D translation and rotation. d Final integration of the maxillary cast and the cephalograms

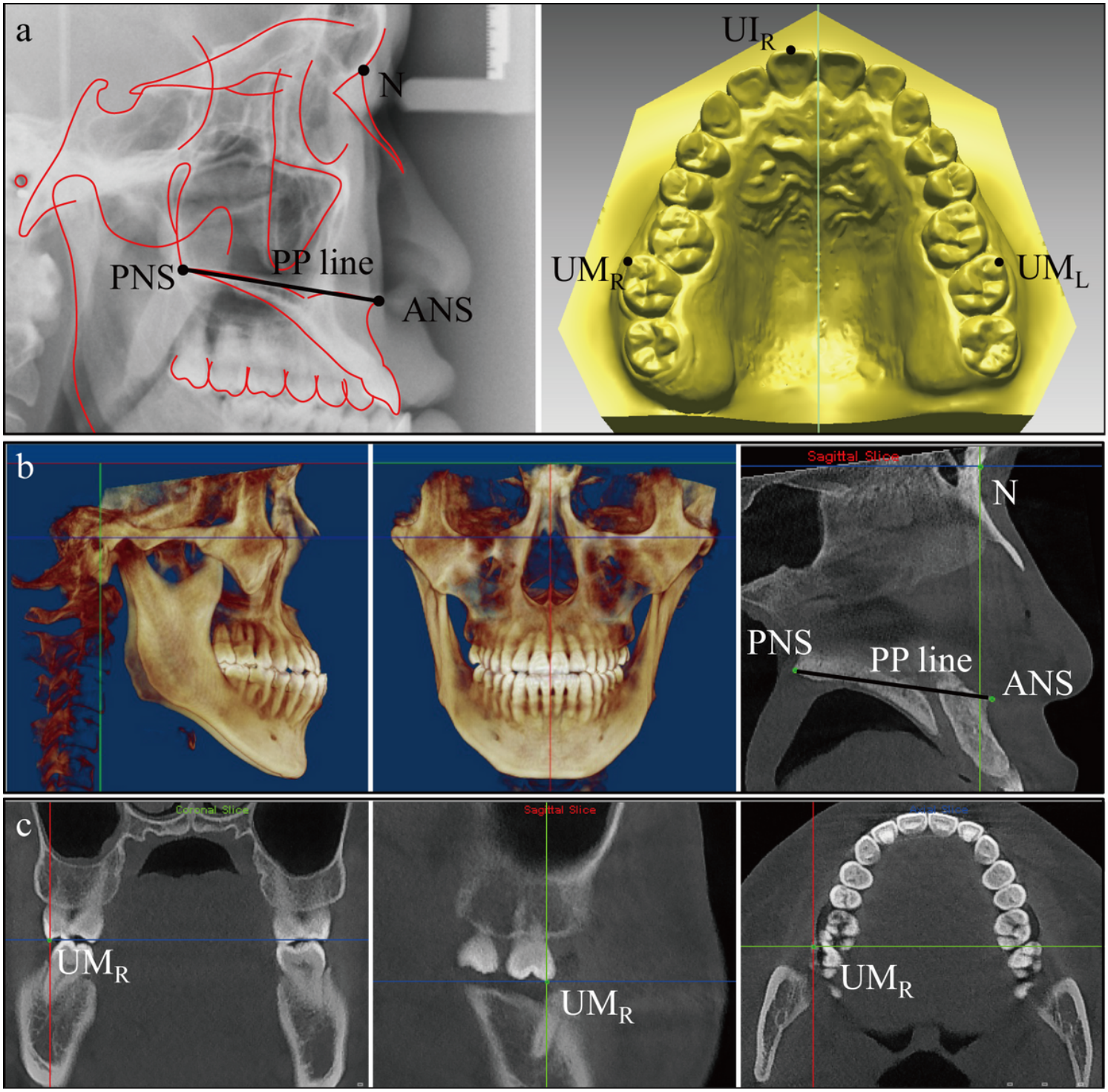

Figure 3

Linear measurements on the integrated images and CBCT. a Nasion (N), ANS, and PNS points were selected on the lateral cephalogram, mesiobuccal cusps of bilateral second molars (UMR and UML) and midpoint of the incisal edge of the right central incisor (UIR) were selected on the dental cast. b The skull was oriented with the Frankfort horizontal plane parallel to the ground along with the midsagittal plane passing through the nasion, sella, and basion points and the landmarks of N, ANS, and PNS were located on the midsagittal plane. c Landmarks of UMR, UML, and UIR were located from coronal, sagittal, and axial planes

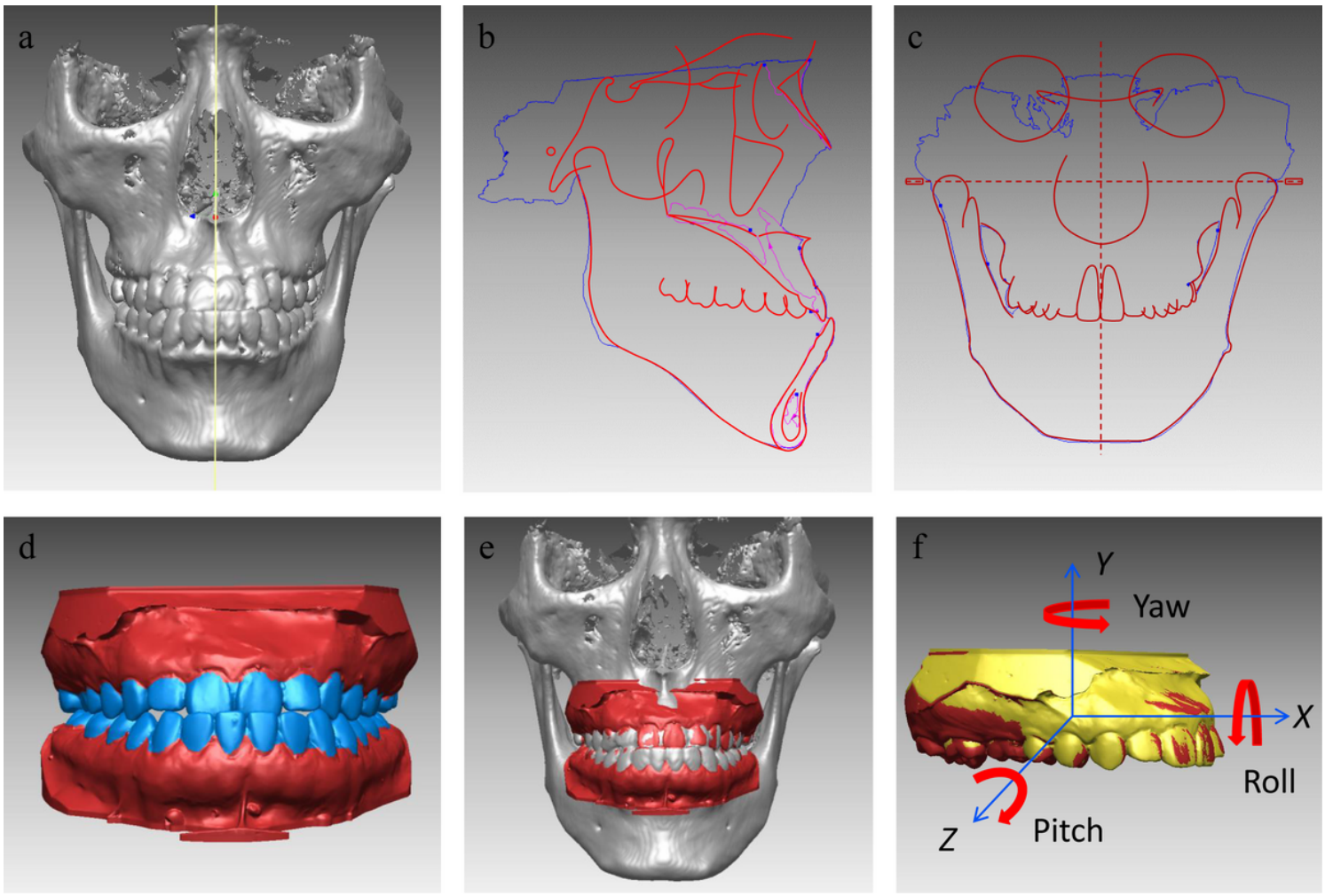

Figure 4

Registration of CBCT and the integrated images for angular measurements. a The mirror symmetry plane of the CBCT model coincided with the XY plane. b-c The sliced (purple) and projected (blue) outline curves of CBCT model conincided with the lateral and frontal cephalogram tracings (red). d-e Superimposition of the copied dental cast and the CBCT model with crown surfaces of all teeth (blue) for registration. f Deviation of the cephalogram-integrated dental cast (yellow) from the CBCT-superimposed dental cast (red) in terms of pitch, roll and yaw

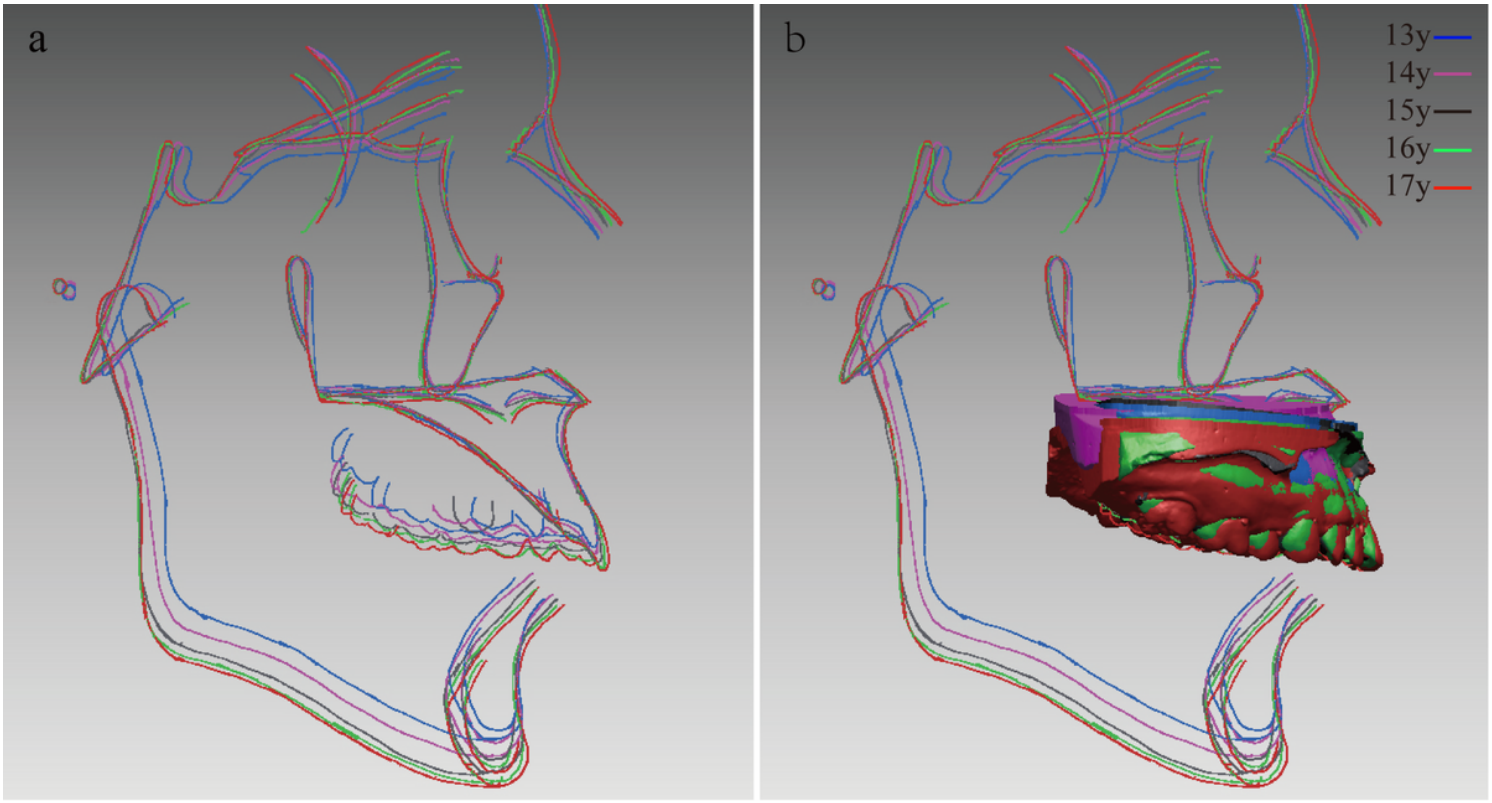

Figure 5

Example of research application of the integration method. a Maxillary structural superimposition of the lateral cephalograms from age 13 to age 17. b Indirect maxillary dental cast superimposition using a combination of the integration method and cephalometric superimposition

Supplementary Files

This is a list of supplementary files associated with this preprint. Click to download.

- additionalfile1.txt
- additionalfile2.txt